Geomorphology 110 (2009) 58–67

Contents lists available at ScienceDirect

Geomorphology

journal homepage: www.elsevier.com/locate/geomorph

Review

Bajada del Diablo impact crater-strewn field: The largest crater field in the Southern Hemisphere

R.D. Acevedo [a,*], J.F. Ponce [a], M. Rocca [b], J. Rabassa [a,c], H. Corbella [d,e]

[a] CADIC-CONICET, c/B.Houssay n°200, 9410 Ushuaia, Tierra del Fuego, Argentina
[b] Mendoza 2779, 1428DKU Buenos Aires, Argentina
[c] Universidad Nacional de la Patagonia-San Juan Bosco, Sede Ushuaia, Argentina
[d] CONICET and Museo Argentino de Ciencias Naturales "Bernardino Rivadavia," Buenos Aires, Argentina
[e] Universidad Nacional de la Patagonia Austral, Río Gallegos, Argentina

ARTICLE INFO

Article history:
Received 25 September 2008
Received in revised form 26 March 2009
Accepted 29 March 2009
Available online 14 April 2009

Keywords:
Impact crater-strewn field
Patagonia

ABSTRACT

Recent remote sensing analyses and field studies have shown that Bajada del Diablo, in Argentina, is a new crater-strewn field. Bajada del Diablo is located in a remote area of Chubut Province, Patagonia. This amazing strewn field contains more than 100 almost circular, crater-type structures with diameters ranging from 100 to 500 m in width and 30 to 50 m in depth. It is composed of three separated impact crater fields, which formed simultaneously. The impact was upon a Miocene basaltic plateau and Pliocene–Early Pleistocene pediments. The original crater field (60 km^2) was later eroded by Late Pleistocene fluvial processes; thus, three major, separate areas were defined. Due to the erosional processes that have affected the area, it is difficult to determine yet if the crater field has a classic elliptical distribution. Crater structures are similar in target rocks, although showing different response and morphology in relation to rock type. They are simple rings, bowl-shaped with raised rimrock. Basaltic boulders have been deposited as a ring-shaped pile and the ejecta are found toward the NE flanks. The craters present a hummocky bottom, with dry ponds and lakes in the center, but they do not show raised central peaks. The rocks within the craters have strong and stable magnetic signature. No meteorite fragments or other diagnostic landmarks have been found yet. The craters have been partially filled in by debris flows from the rim and windblown sands in recent times. The origin of these crater fields may be related to multiple fragmentation of one asteroid that broke up before impact, perhaps traveling across the space as a rubble pile. Alternatively, multiple collisions of comet fragments could explain the formation of these crater fields. Based on field geological and geomorphological data, the age of this event is estimated to be bracketed between Early Pleistocene and Late Pleistocene (i.e., 0.78–0.13 Ma ago).

1. Introduction

During the last 30 years, detailed studies of planets and moons have demonstrated that the impacts of asteroid and comets are the dominant geological and geomorphological processes in the Solar System. The surface of the Moon, Mars, Venus, and Mercury are good examples, being covered by thousands of impact craters. Earth is not the exception. But presently no more than 200 impact craters known today are distributed over all continents. At present, the surface of Earth is being modeled by comet and asteroid impacts.

Concerning meteorite crater-strewn fields on Earth, only a few are known and are shown here in order by number of the impact structures (Table 1).

Bajada del Diablo impact crater field (42°49′ S and 67°28′ W) in central northern Patagonia, Argentina (Fig. 1), is an important feature that should be added to this list. Until today, Bajada del Diablo impact crater field has not been listed in any records of terrestrial crater fields (see: http://www.unb.ca/passc/ImpactDatabase).

2. Regional geology

The Bajada del Diablo impact crater field is located in the Northern Patagonian Massif, also known as the "Meseta de Somun Curá." Most of this ancient massif has remained exposed as a positive craton, uncovered by the sea since the Triassic, and perhaps even since the Late Permian.

The oldest rocks in the region are limestones and shales of the Santa Anita Fm. (Callovian–Oxfordian), which represent the sedimentary infilling of a structural basin developed in Gondwana since the Triassic (Fig. 2). This area was later downwasted and extensive planation surfaces developed under tropical climate. The Araucanian movements of the Andean Cordillera Cycle increased the relief through fault reactivation, overdeepening the basins that controlled the sedimentation of continental epiclastic/pyroclastic rocks of the Chubut Group, during the Albian–Turonian stages (Ardolino and Franchi, 1996).

During the Oligocene and Miocene, the most significant events were the volcanic extrusions, whose first lithological records are the

* Corresponding author. Tel.: +54 2901 422310; fax: +54 2901 430644.
E-mail address: acevedo@cadic.gov.ar (R.D. Acevedo).

0169-555X/$ – see front matter © 2009 Elsevier B.V. All rights reserved.
doi:10.1016/j.geomorph.2009.03.026

Table 1
Meteorite crater-strewn fields on Earth.

#	Name of the impact structure	Geographical location	Geology of the target	Number of craters	References
1	Sikhote Alin	Russia	Jurassic siliceous-clayey rocks	159	Fesenkov, 1958; Divari, 1962; Fisher, 1963; Krinov, 1963, 1966; Nekrasov and Tsvetkov, 1970; Millman, 1970; Krinov, 1971, 1972; Kolesnikov et al., 1972; Tsvetkov, 1972; Shkerin, 1973; Aaloe et al., 1974; Krinov, 1975; Fedynsky and Khryanina, 1976; Kestlane and Tsvetkov, 1987; McHone and Killgore, 1998
2	Chiemgau	Germany	Pleistocene moraines and glaciofluvial gravels	81	Schüssler et al., 2005
3	Campo del Cielo	Argentina	Recent alluvial sands, clays and soils	26	Nágera, 1926; Milton, 1964; Cassidy et al., 1965; Bunch and Cassidy, 1968; Cassidy, 1968; Villar, 1968; Cassidy, 1971; Traub and Cassidy, 1989; Cassidy and Renard, 1996; Cassidy and Wright, 2003; Wright et al., 2007
4	Gilf Kebir	Egypt	Upper Cretaceous sandstones	13	Paillou et al., 2004
5	Henbury	Australia	Precambrian sandstones (Winnall Beds sub-greywackes) 730 my ±45 Ma Rb/Sr	13	Alderman, 1931; Spencer and Hey, 1933; Rayner, 1939; Taylor and Kolbe, 1964, 1965; Hodge, 1965; Milton and Michel, 1965; Taylor, 1965, 1966, 1967; Milton, 1968; Compston and Taylor, 1969; Hodge and Wright, 1971; Milton, 1972; Axon and Steele-Perkins, 1975; Simmons, 1975; Taylor and McLennan, 1979; O'Keefe, 1980; McColl, 1990, 1997
6	Kaalijärv	Estonia	Lower Silurian dolomites	9	Krinov, 1961; Aaloe and Tiirmaa, 1982; Lyakhovitskiy and Guklengov, 1987; Marini et al., 2004
7	Morasko	Poland	Quaternary and Neogene sediments	8	Bartoschewitz, 2002
8	Wabar	Saudi Arabia	Recent dune sands	4	Philby, 1933; El-Baz and El Goresy, 1971; Shoemaker and Wynn, 1997; Wynn and Shoemaker, 1997; Wynn, 2002

tuffs of the Sarmiento Group. The most relevant Cenozoic volcanism is represented by the Oligocene lava flows of the Somún Curá Fm., which formed the extensive plateau of this name (Fig. 2). The stratigraphic position between these two latter units indicates the existence of interbedding of both units (Ardolino, 1987). The central eruptions of lavas and pyroclastic rocks during the Oligocene were also important, generally of trachytic, rhyolitic, trachyandesitic, and trachybasaltic composition (Quiñelaf Eruptive Complex) of the Sierras de Apas and Sierras de Telsen. As a consequence of the Pehuenche Phase of the Andean Cycle, a deep reorganization of the different regional blocks took place. The disintegration of the highest mountain blocks under an arid/semiarid cold climate (Sierras de Apas, Telsen, and Chacays) produced a great amount of gravelly and sandy debris that was deposited in the shape of mantles forming the topmost portion of the main tableland (Pampa Sastre Fm., Pliocene–Early Pleistocene; Fig. 2). The rest of the Pleistocene was characterized by a general elevation of the area, with a relative lowering of base level. Consequently, erosive and sedimentary processes generated three accumulation surfaces around the core of this ancient massif (Ardolino and Franchi, 1996).

In structural terms, this region is characterized by block tectonics that, under the influence of various movements, formed uplifted and depressed areas, controlling sedimentation since the Jurassic until today. Main, NE–SW fracture alignments have been determined (Ardolino and Franchi, 1996).

3. Geomorphology

The geomorphological features of this region are basically derived from fluvial, colluvial, and other mass wasting processes, although

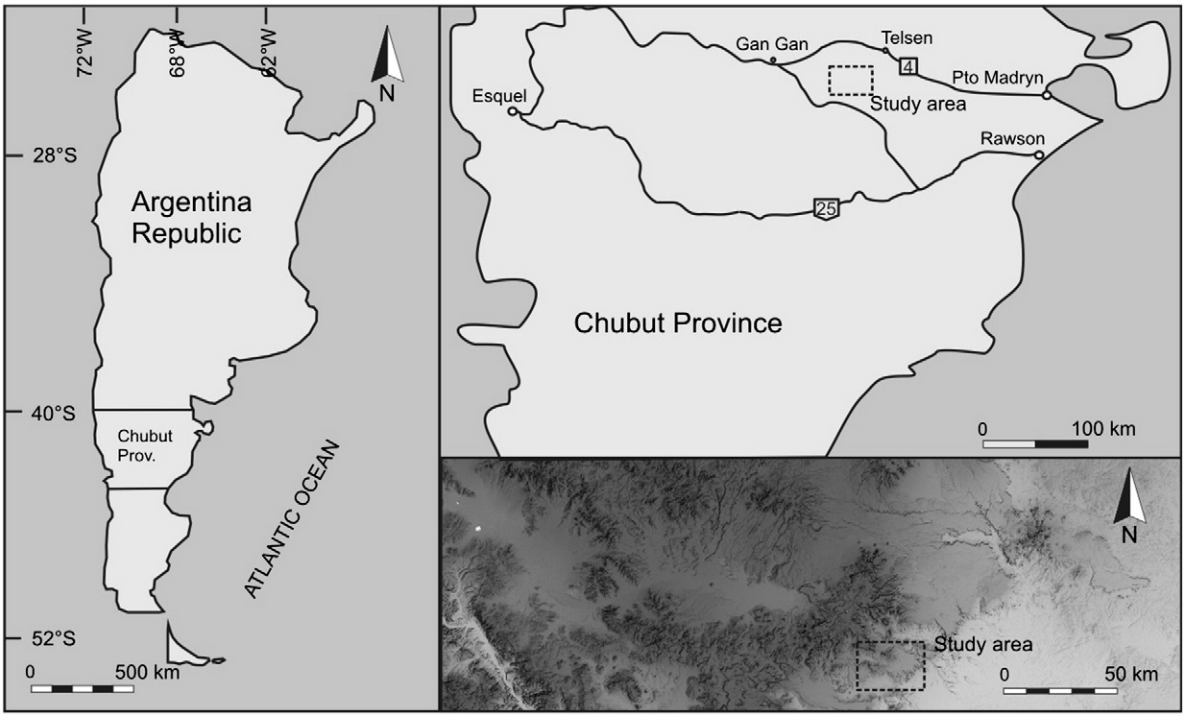

Fig. 1. Location map. The inset shows a satellite image of the study area.

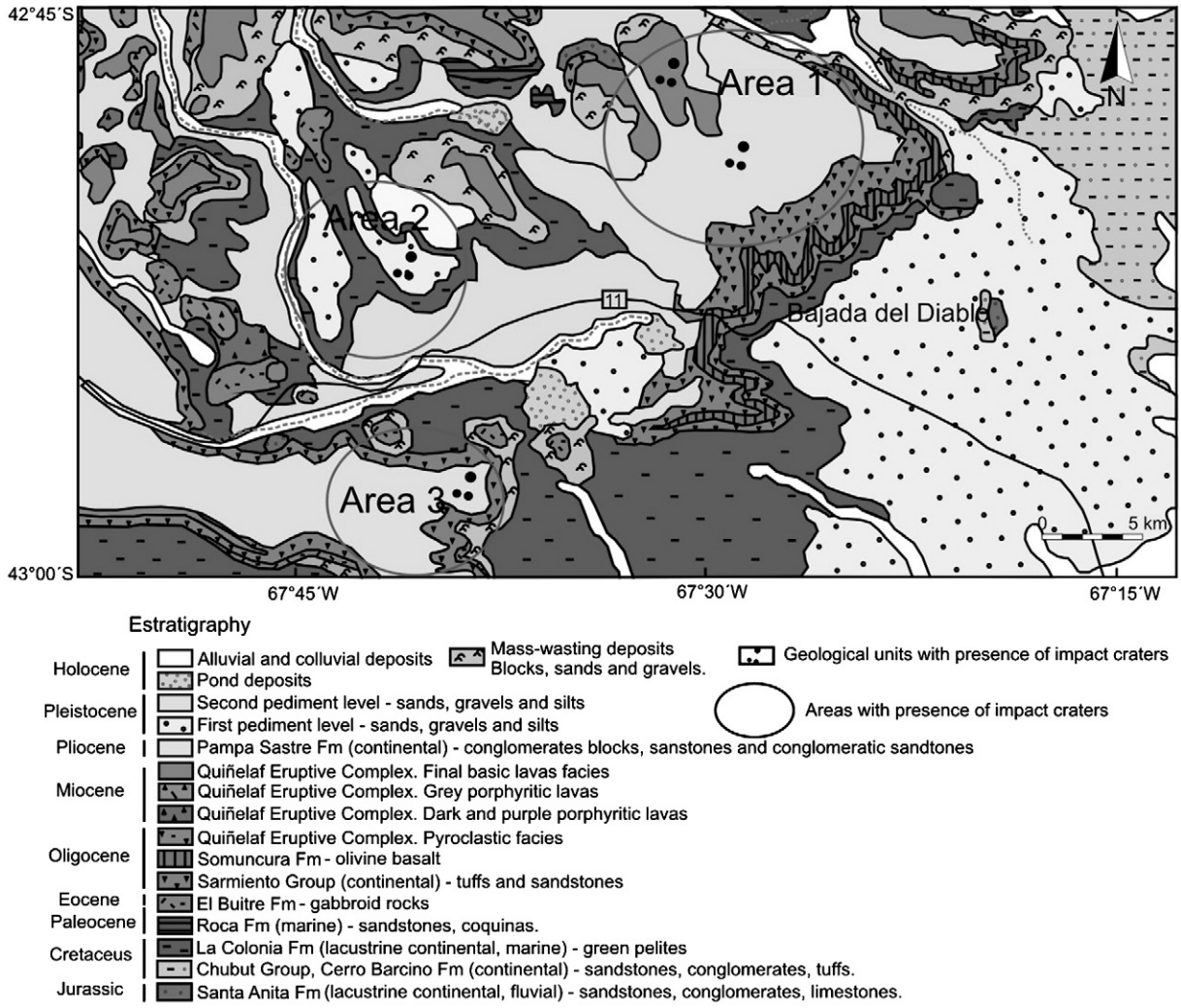

Fig. 2. Regional geological map of the Bajada del Diablo area. All stratigraphical units present in the area are depicted in the accompanying chart.

Tertiary volcanic activity has developed unique characteristics as well. The main geomorphological feature in the area is a volcanic structural plateau. Abrupt sides are bounding a high, regular surface above the nearby lands. The tableland is composed of an extensive Cenozoic lava plateau, formed of successive flows that expanded over an approximately flat relief eroded mostly on friable rocks. In the high cliffs, up to 200 m of usually very soft clastic rocks may be observed (La Colonia Fm. and Chubut Group), in some areas covered by two basaltic mantles (the lower one corresponding to the Somún Curá Fm. and the upper one to the Quiñelaf Eruptive Complex) with tuffaceous intercalations (Ardolino and Franchi, 1996).

The exogenous cycle has highlighted the areas occupied by the more resistant lavas, eliminating the friable materials. Ardolino (1987) named this geomorphological unit as a structural tableland, whereas González Díaz and Malagnino (1984) classified the Somún Curá Meseta as a volcanic structural plain. The upper portion of the "meseta" (that is, a tableland) is a smoothly undulating surface which rises towards the northwest.

4. Principal lithological characteristics of the rock units and landforms showing impact craters at Bajada del Diablo

Two rock types exist in the study area on which impact craters have been observed (Fig. 3).

4.1. Quiñelaf eruptive complex

Most of the rocks forming the Quiñelaf Eruptive Complex have been classified as trachytes, but other rocks are present, such as rhyolites, trachyandesites, trachybasalts, and pyroclastic rocks. Ardolino (1981, 1987) presented a division of this complex in various facies: Pyroclastic Facies, Lava Facies (acid lavas, dark porphyritic lavas and grey and purple porhyritic lavas), Intrusive Facies (dykes and intrusive bodies), and Final Lava Facies. Several of the craters found at Bajada del Diablo, placed in this latter facies, are dark grey, porphyritic, olivine basalts, with an affanitic mass in which light-colored felspar and reddish mafic phenocrysts are found.

On the basis of several radiometric datings, Ardolino (1981) identified that the latest volcanic activity of this trachytic unit (the Final Lava Facies) took place in the Miocene.

4.2. Pampa Sastre Formation

This unit is a sandy, gravelly complex located on top of the tablelands. At Bajada del Diablo, these rocks appear on top of the Sarmiento Group tuffs. They are conglomerate layers with dominant basalt clasts, which increase their size upward, with petrocalcic interbedded layers. In the upper portion, the clasts are boulder size, in a brownish, coarse sandy matrix cemented with Ca carbonate. They

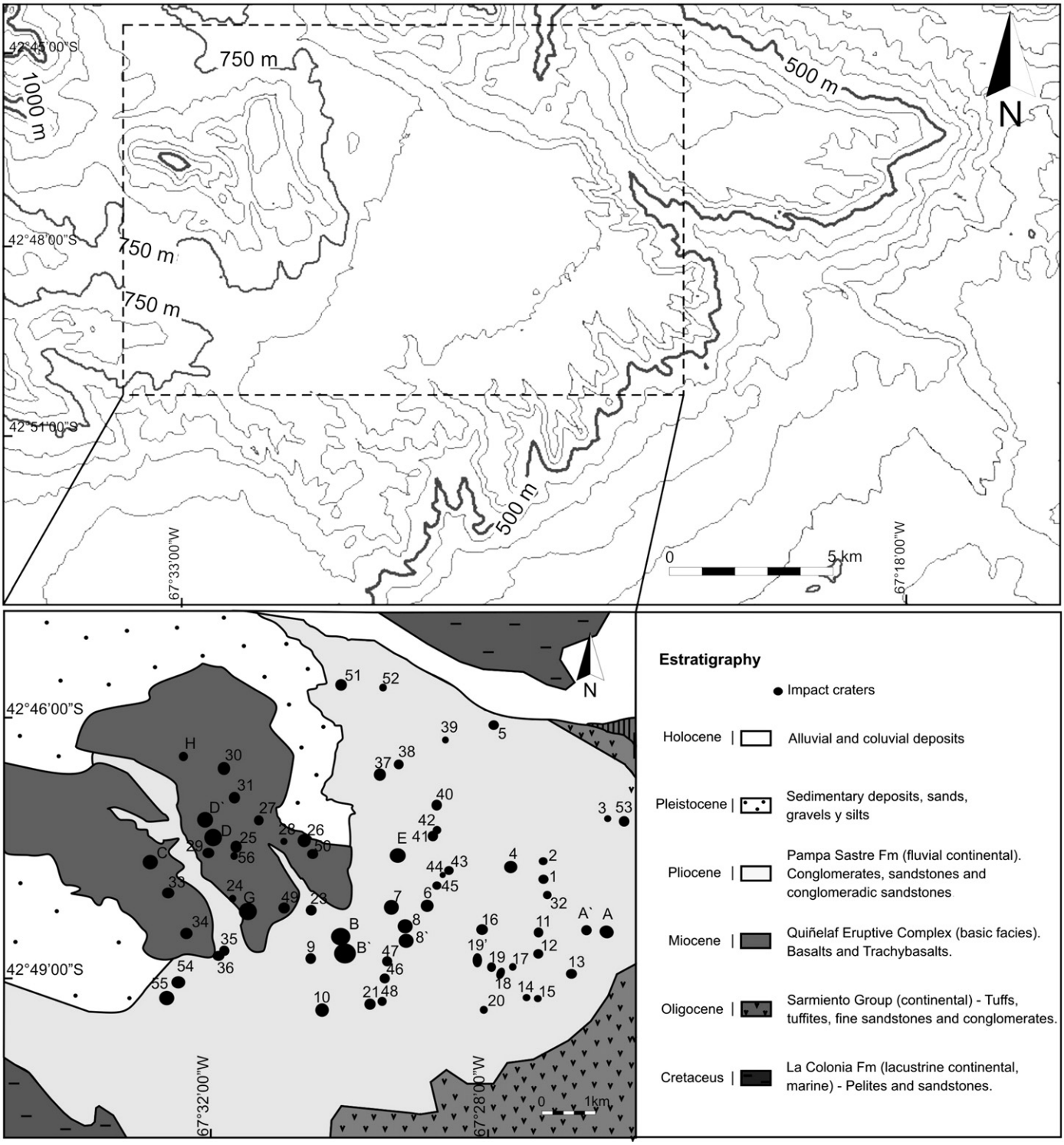

Fig. 3. Detailed geological and geomorphological map of the Filu-Có Plateau, Bajada del Diablo area. The black circles represent the observed craters, with the diameters represented at scale. The existing geological and geomorphological units were surveyed during fieldwork. Many craters occur on the basaltic tablelands and piedmont landforms.

form fluvial deposits and are part of piedmont and talus landforms, generally as a result of the erosion of volcanic rocks from the Sierras de Apas, Chacays, and Telsen. These sediments are compositionally and texturally very immature, showing a short and fast transportation.

These compositions, basically being clasts of Middle Miocene volcanic rocks (basalts, olivine basalts, trachytes, olivine trachytes, trachybasalts, etc.), allow us to assign a Pliocene–Early Pleistocene age to these units (Ardolino and Franchi, 1996).

5. Impact crater-strewn field

Twenty years ago, one of the present authors (Corbella, 1987), who was working on the petrology of alkaline rocks of the Bajada del Diablo area, suggested that at least more than 100 local landforms, essentially circular hollows and depressions, could be the result of meteoritic impact. No further research investigated this hypothesis. Based on this pioneer information, fieldwork was carried out in May 2007 by some of

Table 2
Localization of craters on Filú-Có plateau.

Crater	Latitude	Longitude	Diameter	Impacted lithology
A	42° 48′ 27.7″	67° 26′ 10.10	220 m	Sandstones and conglomerates (PSF)
A'	42° 48′ 27.36″	67° 26′ 27.64″	165 m	"
B	42° 48′ 16.67″	67° 30′ 15.63″	351 m	"
B′	42° 48′ 27.5″	67° 30′ 11.7″	271 m	"
C	42° 47′ 18.9″	67° 32′ 54.11″	270 m	Basalts and trachybasalts (QEC)
D	42° 47′ 04.8″	67° 31′ 59.8″	278 m	"
D′	42° 46′ 54.96″	67° 32′ 05.3″	219 m	"
E	42° 47′ 27.79″	67° 29′ 23.05″	355 m	Sandstones and conglomerates (PSF)
G	42° 47′ 55.67″	67° 31′ 34.45″	291 m	Basalts and trachybasalts (QEC)
H	42° 46′ 13.48″	67° 32′ 19.61″	146 m	"
1	42° 47′ 50.8″	67° 27′ 09.2″	168 m	Sandstones and conglomerates (PSF)
2	42° 47′ 39.6″	67° 27′ 08.1″	154 m	"
3	42° 47′ 16.9″	67° 25′ 48.7″	170 m	"
4	42° 47′ 41.19″	67° 27′ 36.3″	241 m	"
5	42° 46′ 04.6″	67° 27′ 44,5″	152 m	"
6	42° 48′ 00.8″	67° 28′ 56.8″	212 m	"
7	42° 48′ 00.17″	67° 29′ 30.5″	237 m	"
8	42° 48′ 14.5″	67° 29′ 18.3″	245 m	"
8′	42° 48′ 25.9″	67° 29′ 16.9″	259 m	"
9	42° 48′ 30.9″	67° 30′ 44.2″	176 m	"
10	42° 49′ 04.2″	67° 30′ 36.08″	239 m	"
11	42° 48′ 24.7″	67° 27′ 18.5″	129 m	"
12	42° 48′ 39.6″	67° 27′ 18.5″	189 m	"
13	42° 48′ 55.8″	67° 26′ 46.21″	174 m	"
14	42° 49′ 09.0″	67° 27′ 35.6″	117 m	"
15	42° 49′ 12.21″	67° 27′ 19.7″	110 m	"
16	42° 48′ 20.73″	67° 28′ 06.67″	170 m	"
17	42° 48′ 47.33″	67° 27′ 41.23″	112 m	"
18	42° 48′ 49.33″	67° 27′ 52.07″	122 m	"
19	42° 48′ 46.31″	67° 28′ 01.53″	176 m	"
19′	42° 48′ 41.49″	67° 28′ 13.63″	186 m	"
20	42° 49′ 14.62″	67° 28′ 12.69″	114 m	"
21	42° 48′ 59.32″	67° 29′ 55.22″	159 m	"
23	42° 47′ 58.8″	67° 30′ 41.59′	237 m	"
24	42° 47′ 46.32″	67° 31′ 47.02″	145 m	Basalts and trachybasalts (QEC)
25	42° 47′ 12.72″	67° 31′ 42.11″	197 m	"
26	42° 47′ 12.15″	67° 30′ 42.77″	218 m	"
27	42° 46′ 56.63″	67° 31′ 22.04″	146 m	"
28	42° 47′ 10.08″	67° 31′ 01.53″	104 m	"
29	42° 47′ 16.22″	67° 32′ 03.83″	175 m	"
30	42° 46′ 23.5″	67° 31′ 46.13″	217 m	"
31	42° 46′ 40.69″	67° 31′ 42.30″	229 m	"
32	42° 48′ 01.12″	67° 27′ 03.03″	161 m	Sandstones and conglomerates (PSF)
33	42° 47′ 38.45″	67° 32′ 41.41″	201 m	Basalts and trachybasalts (QEC)
34	42° 48′ 06.27″	67° 32′ 28.51″	176 m	Basalts and trachybasalts (QEC)
35	42° 48′ 19.24″	67° 31′ 57.37″	181 m	Sandstones and conglomerates (PSF)
36	42° 48′ 23.16″	67° 32′ 00.91″	201 m	"
37	42° 46′ 34.95″	67° 29′ 35.27″	200 m	"
38	42° 46′ 27.51″	67° 29′ 14.92″	141 m	"
39	42° 46′ 14.57″	67° 28′ 34.52″	75 m	"
40	42° 47′ 56.93″	67° 28′ 47.78″	210 m	"
41	42° 47′ 21.57″	67° 28′ 53.70″	152 m	"
42	42° 47′ 17.85″	67° 28′ 47.73″	125 m	"
43	42° 47′ 39.20″	67° 28′ 39.34″	148 m	"
44	42° 47′ 43.96″	67° 28′ 42.30″	60 m	"
45	42° 47′ 49.73″	67° 28′ 48.23″	84 m	"
46	42° 48′ 35.5″	67° 29′ 45.59″	170 m	"
47	42° 48′ 33.48″	67° 29′ 37.94″	225 m	"
48	42° 48′ 59.22″	67° 29′ 44.76″	152 m	"
49	42° 47′ 56.84″	67° 31′ 09.97″	180 m	Basalts and trachybasalts (QEC)
50	42° 47′ 21.37″	67° 30′ 37.94″	211 m	"
51	42° 45′ 24.49″	67° 30′ 13.41″	198 m	Sandstones and conglomerates (PSF)
52	42° 45′ 26.91″	67° 29′ 41.57″	120 m	"
53	42° 47′ 19.25″	67° 25′ 52.28″	225 m	"
54	42° 48′ 48.65″	67° 32′ 51.49″	220 m	"
55	42° 48′ 39.21″	67° 32′ 39.21″	230 m	"
56	42° 47′ 19.97″	67° 31′ 43.20″	110 m	Basalts and trachybasalts (QEC)

PSF: Pampa Sastre Formation; QEC: Quiñelaf Eruptive Complex. Letters indicate the craters actually surveyed in the field. Numbers indicate those which were identified and measured on aerial photographs.

the present authors (R.D.A., J.F.P., and J.R.) in an attempt to verify such an hypothesis for these features in a very remote region of central Patagonia.

The locality of Bajada del Diablo (meaning "Devil's slope") is located at 42°52′ S, 67°28′ W, 500 m a.s.l., in the central part of Chubut Province (Argentina), and around 120 km SE of the small village of Gan-Gan, the nearest inhabited site (Fig. 1).

This large meteorite crater-strewn field, covering an area of about 90 km^2 between 42°44′ to 42°51′ S and 67°36′ to 67°24′ W, contains >100 impressive circular and subcircular crater-like landforms with diameters ranging from 60 to 350 m in width, 30 to 50 m in depth, and distributed in three separated areas (Table 2).

The Bajada del Diablo strewn field, composed of three separated impact crater fields, does not seem to present a classic elliptical distribution, probably due to the erosional fluvial processes that took place in the area after the impact, masking the original distribution. Nevertheless, the nature and field geomorphological relationships of these features indicate that craters are temporally correlated and that they were most likely formed simultaneously. Weathering, erosion, and burial (infilling by eolian sediments) processes have slightly modified the original shapes. The preservation of the craters is quite different depending on location. The crater field has been partially eroded by Late Pleistocene fluvial processes. Some of the original

Table 3
Number of craters identified, impacted area, and crater density.

Zone	Area (km^2)	Number of craters	Crater density (craters/km^2)
1	80	66	0.825
2	32	12	0.37
3	44	15	0.34

Zone 1 is the Filu-Có Plateau; zones 2 and 3 refer to other unnamed areas. A fourth area is present but it has not yet been studied.

craters have been eliminated by erosion, mostly fluvial incision. Thus, three major, separate areas are defined today. The estimated crater density of these areas is shown in Table 3.

The total number of craters that would have formed during the impact event, and which existed before the Late Pleistocene erosion cycle took place, has been estimated at a minimum of 206, based on the average density of the three impact zones (0.6 craters/km^2) and the minimum total impact area estimated between the three impact zones (398 km^2). Other craters may be present, but proper identification would need more extensive fieldwork in this very remote area. Notably, the densities observed in zones 2 and 3 were estimated based only on the interpretation of satellite imagery of low spatial resolution because no aerial photographs are yet available for these areas. In zone 1, instead, aerial photographs were used and field checking was accomplished. This would explain the significant differences between estimated densities in between these zones. Thus, the estimated number of original craters should be considered only as a minimum.

The first studied area is on the Filu-Có Plateau, which is located in a more northeasterly position in relation to the other two. This locality is composed of (i) a volcanic plateau of Late Miocene basalts and trachybasalts of the Quiñelaf Volcanic Complex, (ii) coarsely stratified sedimentary breccias, conglomerates, and sands of the Pampa Sastre Fm., a Late Pliocene–Early Pleistocene pediment which extends around most of it, and (iii) Late Pleistocene fluvial deposits forming terraces and network channels (Ardolino and Franchi, 1996).

The Filu-Có area includes at least 66 impact craters found on the Miocene plateau and the Late Pliocene/Early Pleistocene pediment, but craters are absent on the younger Pleistocene fluvial landforms. The observation of satellite images shows central dots at the center of most craters (Fig. 4, craters D and G). They are not raised central peaks, however, as could be expected, but dry lake surfaces instead. Crater landforms are similar in both target rocks, the Miocene basalts, and the Late Pliocene/Early Pleistocene sediments, although they show several differences. The preservation of the craters thus varies depending upon the impacted rocks.

Two other areas with craters, mentioned in Corbella (1987), and possibly a fourth area are located south and southwest of the Filu-Có Plateau. These neighboring areas have been surveyed on the satellite imagery, but they have not been studied in the field yet.

6. Craters on the Miocene basalts

At least 18 craters have been found on top of the Miocene basaltic plateaus at Bajada del Diablo (Fig. 5). These volcanic mesas were formed by basalt lava pouring out from local volcanoes during the Late Miocene and becoming later a positive feature because of landscape inversion (Ardolino and Franchi, 1996). These volcanic tablelands were already positive landscape features, perhaps a few tens of meters above the local network channels then, when the impacts took place. The local relief today is roughly around 100 m. Some of the impact structures have been cut by subsequent, Late Pleistocene fluvial and backward erosion at the margins of the volcanic tableland, as shown by some of the craters depicted in Fig. 5.

The crater morphology corresponds to bowl-shaped inner areas surrounded by a more or less continuous ring wall and a hummocky outer surface that are gently sloping away from the ring wall. The interior wall usually has a slope of 30° to 20°, whereas the outer wall is irregular with basaltic rubble made up of boulder-sized, angular fragments. In agreement with the models of Melosh and Ivanov (1999) they are simple rings, bowl-shaped with a raised rimrock. Depth is 20 m for the small (140 m) and almost perfectly circular H crater (Chappelow and Sharpton, 2002). The ring walls were originally closed, but they exhibit today a few gaps from erosion and mass-movement processes. The ejecta are found only toward the NE flanks of the ring walls. Unfortunately, no meteorite fragments or other megascopic diagnostic landmarks have been found yet among the boulders and pebbles of vesicular basalt.

7. Craters on the pediment surface

Craters on the pediment surface are simple rings, bowl- to smooth-shaped with raised to flat shores. Depth field estimations are between 20 m for crater B (diameter 270 m) and almost none for crater A (diameter 220 m). The shores match exactly a circular shape. They present a hummocky bottom, with dry ponds and salt lakes in the center. Later, they were dewatered and filled up with gravel and sand. As a consequence of the obliteration and burial, they may be difficult to recognize. The rocks found within the craters have strong and stable magnetic signature. The craters have been partially filled in by debris flows from the rim and wind-blown sands in recent times. Ejecta are commonly strongly marked in the satellite imagery (see Figs. 4 and 5).

8. Nickel-bearing sands

In the interior of two horseshoe-shaped twin craters (both with ejecta), nickel (Ni) anomalies were detected (Fig. 4, craters A and A'). Chemical analyses were performed on sands and silts found at the bottom of the craters. A small portion of the magnetic sand was mixed with one drop of 1% dimethylglyoxime ($C_4H_8N_2O_2$) in 10% hydrocloric acid solution, and eight drops of ammonia were added. The coloration of liquid turned reddish, indicating the presence of nickel, as the acid dissolved the metallic phase releasing nickel ions in solution. This positive Ni test is common among basaltic debris but also suggests a possible meteoritic origin as remnants of the impactor. Nickel analyses from surrounding sediments outside the crater do not show this Ni anomaly. In addition, X-ray diffraction studies have shown the presence of magnetite and petrogenic silicates, such as felspars and plagioclases, and also the possibility of taenite, a rare Fe–Ni mineral.

9. Discussion

The locality of Bajada del Diablo displays an unusual geological feature in which field geological and geomorphological data, petrographical evidence, and stratigraphic modifications support the interpretation of an impact origin for these circular structures, according with the parameters of O'Keefe and Ahrens (1999). Bajada del Diablo target material consists of basalt rocks and overlying unconsolidated soft sediments. We suggest, therefore, that these craters were formed by the impact of a fragmented extra-terrestrial projectile. Over 100 circular structures have been identified, so far, in satellite imagery and 10 of them were actually surveyed in the field.

The large number of craters, the morphology, and the existence of oriented fans of debris and ejecta provide a strong argument and unambiguous evidence for an impact origin.

Positive Ni tests may be indicative of the presence of either a chondritic or an iron meteoritic component in the debris, which may contain a small but measurable amount of the impactor.

The origin of these crater fields may be related to multiple fragmentation of one stony and (or) iron asteroid that broke up before impact, traveling across space as a rubble pile type of asteroid.

When entering the atmosphere of Earth, the impactors were projected in a theoretical shallow input angle between 15° and 25° from the horizontal from the SW, smashing against the surface. With the ejecta blanket mainly developed on the NE rim of the craters, clear evidence exists for a quite oblique impact angle because on larger impact angles the ejecta blanket is distributed all around the impact crater and not on a particular area.

The layout of the ejecta that moved preferably in the downrange direction indicates a high velocity impactor. The bearing of this trajectory is SW-to-NE. Evidence shows that the average diameter of

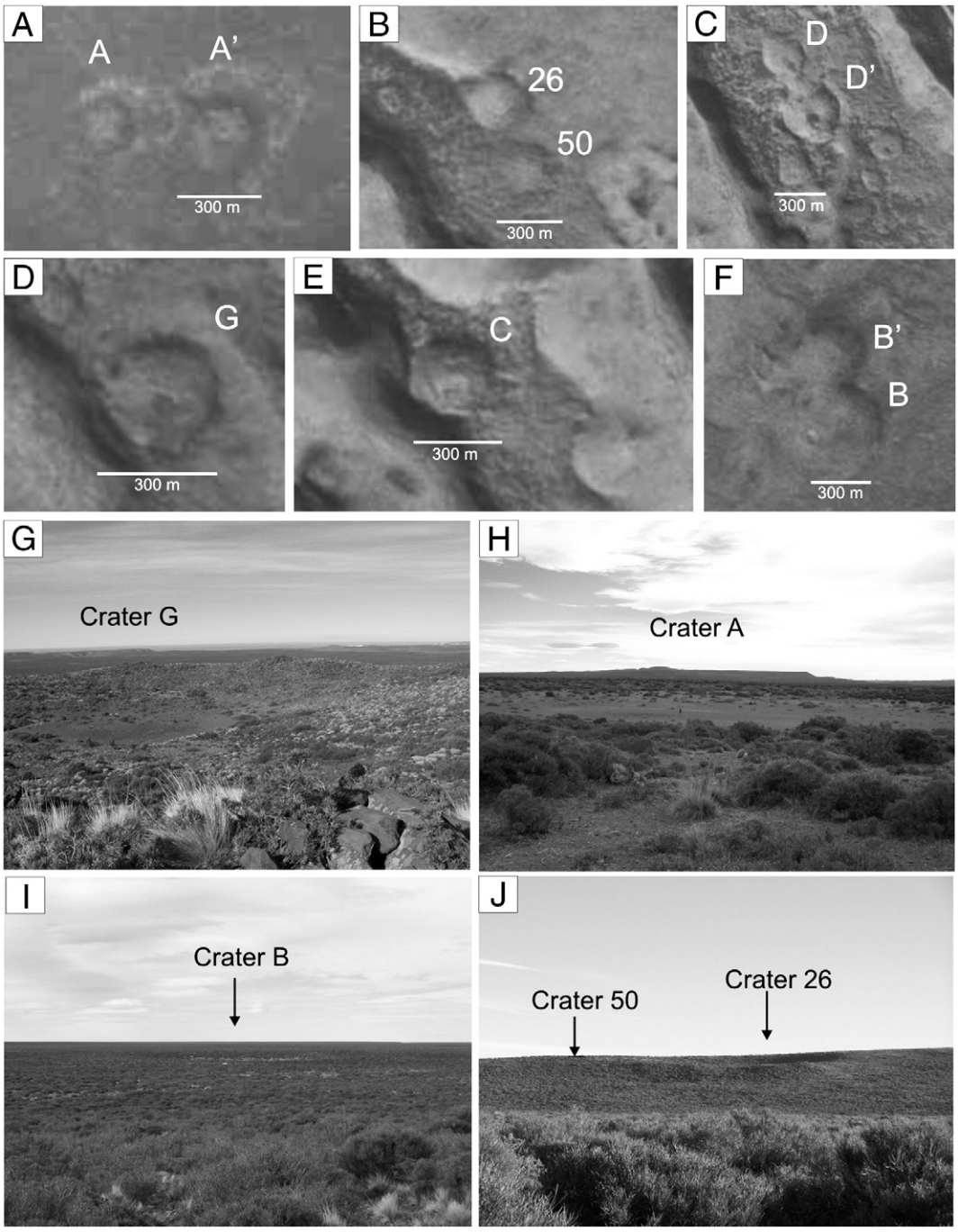

Fig. 4. Different craters at Bajada del Diablo crater strewn field. Craters (A), (F), (H), and (I) are on the piedmont surface; craters (B), (C), (D), (E) (G), and (J) are on the Miocene basalts. Nickel anomalies in A and A' craters [(A) and (H)]; craters in (J) are eroded by headward erosion.

the craters does not increase from the southern to the northern end of the strewn field, which would have been related to an atmospheric breakup of the impactor, thus implying a rough grading of the fragments and of the diameters of the associated craters. Therefore, the idea of a rubble-pile could be most appropriate to explain this chaotic distribution. The absence of meteoritic fragments suggests that the projectile (or rubble pile) was mostly, if not absolutely, vaporized as a result of very high temperature released during such hypervelocity impact. Alternatively, multiple collisions of comet fragments could explain these conditions.

Whereas further field work will certainly reveal additional impact craters, the available aerial photographs, satellite imagery, and field data prove that the observed craters are of impact origin. The most significant diagnostic facts are the almost identical and simultaneous impact craters on volcanic rocks and piedmont sedimentary deposits and the ubiquotuous presence of ejecta fans in all craters, always located on the same side of the depressions. Alternative origins (such as deflation hollows or volcanic, hydrothermal, or phreato-volcanic eruptions) should be ruled out because of the lack of specific features related to these processes. On the other hand, and because the craters formed on different lithologies, the possibility of their origin due to sink-hole processes was excluded also. Finally, human-made origin by aerial bombing is impossible since the area was never bombed, being also incompatible due to their larger size.

The original total population of impact craters at Bajada del Diablo may be estimated by means of the amount of still-visible craters and

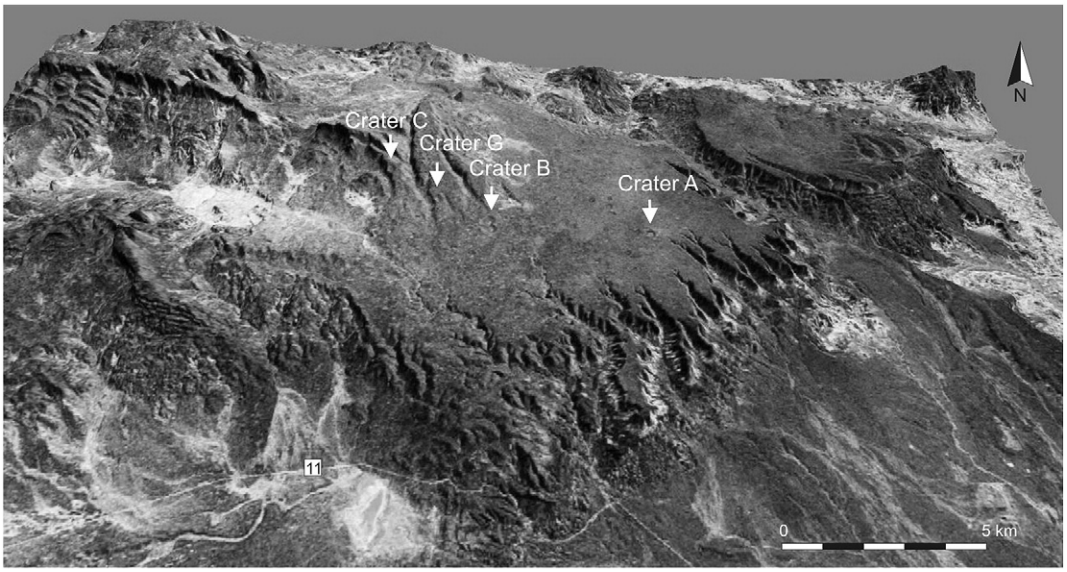

Fig. 5. 3D view of the study area with a vertical exaggeration of 3.75 based on SRTM3 digital model (S43W068.HGT) + Landsat ETM + bands 7, 4, and 2 (S-19-40_2000.SID), using Global Mapper V8.03

the total area originally impacted. Because of recent fluvial erosion, the partial destruction of some of them may be established. Even after severe fluvial erosion, more than 100 surviving craters still exist at Bajada del Diablo. This is a very large amount when compared to other known impact crater fields around Earth (see Table 1). If we take into consideration that the craters are found over an area of 27 by 15 km (a total area of around 400 km^2) and based upon the study and interpretation of satellite imagery and aerial photographs of the crater concentrations that are still visible, the original crater population may be estimated as having a range of 200 to 300.

When a meteorite fall hits the ground, the cosmic particles are distributed in an area defined as the dispersion ellipse. This dispersion ellipse has been observed in most of the impact crater fields known on Earth. The longest axis of the ellipse is always coincident with the movement direction of cosmic bodies. In these cases, the larger craters and those surviving more massive meteorites are found located at one of the ends of the largest axis of the dispersion ellipse. Curiously, no clear evidence has been observed for ellipse dispersion at Bajada del Diablo. Large and small craters seem to be mixed in a random manner in all three crater groups visible in the area.

The absence of a well-defined dispersal ellipse at Bajada del Diablo may be interpreted in four ways:

(i) The model is restricted due to incomplete identification on the ground (that is, the ellipse exists but is not visible).
(ii) Most of the original dispersal ellipse has been erased by fluvial erosion after the impact.
(iii) The impactor object was an asteroid of the "rubble pile" type. Many asteroids are not monolithic, but instead they are formed by a conglomerate of rocks united only by the mutual and weak gravity attraction. These are rock conglomerates of weak or absent internal cohesion. This is the case of the 25143 Itokawa asteroid, recently studied by the Hayabusa Japanese sound (Fujiwara et al., 2006). An asteroid of the "rubble pile" type, when approaching Earth, would be fragmented into hundreds of pieces upon entering the atmosphere because of the effect of terrestrial gravity forces. In this study case, after the breakup of the asteroid, the individual rocky pieces would have impacted the surface, thus creating the Bajada del Diablo crater-strewn field. In this case, this crater distribution would be random and lack a defined dispersion ellipse.
(iv) The extra-terrestrial object that impacted this region could as well have been a small comet nucleus. Comet nuclei, formed by water and carbon dioxide ice, are generally very fragile and tend to break into smaller pieces when they are under the influence of the gravitational attraction force of a major object, such as a planet (Campins and Fernández, 2002; Festou et al., 2004).

Therefore, we hypothesize that the object that impacted at Bajada del Diablo could have been a comet nucleus, several hundred meters in diameter, which fragmented into hundreds of pieces shortly before hitting the surface. The crater distribution also would have been random and lacked a dispersal ellipse. No meteorite fragments have been found yet within or around the studied craters that would support this hypothesis. If the impacting object was an ice-comet nucleus, the fragments would have disappeared very fast, leaving no physical traces behind.

Thus, given the lack of meteoritic material and the irregular ellipse of scattered debris, we suggest that the impacting body was more likely a comet fragment with a relatively small fraction of rocky matter rather than a solid fragment of an asteroid.

10. Conclusions

The Bajada del Diablo crater field is among the largest crater fields on Earth when the total amount of craters identified there as well as the extent of the covered area are considered.

A highly noteworthy aspect of the Bajada del Diablo crater field is that some of the impact craters are located on top of basaltic rock plateaus. This circumstance makes them highly interesting as a matter of comparison with the surface of other planets. The surfaces of the Moon, Mars, Venus, and Mercury are covered by impact craters located on basaltic rock. Until now, only one impact crater on basaltic rock has been recognized on Earth: the Lonar Lake impact in India (Fredriksson et al., 1973). The high number of craters found on basalt at Bajada del Diablo (at least 18) would greatly enhance this evidence.

The Bajada del Diablo impact field could then, perhaps, provide evidence for dozens of impacts on basaltic rocks, and the detailed investigation would generate very valuable information for the study of craters on basalts on other bodies in the Solar System.

Based on the available field geological and geomorphological data, the age of this event is estimated to be bracketed between the Late Pliocene/Early Pleistocene and the Late Pleistocene, based upon the regional stratigraphy and morphochronology. Therefore, the impact likely took place during the Middle Pleistocene (ca. 0.8–0.13 Ma), which agrees with the observed high degree of landform preservation.

Though no meteoritic fragments have been found so far in these areas, the origin is proven by the evidence of simultaneous impacts on volcanic and sedimentary rocks, and the existence of debris ejecta fans always located on the same side of the craters (NE), which suggests a SW–NE trajectory of the projectile. No evidence for alternative origins for these depressions (such as deflation or volcanic or geothermal processes) has been yet found.

Pseudo-central peaks are astonishing features in satellite imagery but their actual absence is coherent with the hypothesis of Pike (1980) respect to simple-to-complex transition for impact craters in Mars.

How can craters be so circular given that the impactors strike Earth's surface at an angle? It is all down to the amount of explosive energy that vaporises everything at the point of impact in a symmetrical circular pattern. The energy of the impact produces an approximately spherical expanding envelope of hot gas, thus generating the crater.

The Bajada del Diablo impact crater field deserves further detailed studies and discussion on its origin, mechanics, and preservation. These objectives will be accomplished in forthcoming fieldwork seasons.

Acknowledgements

This research project has been partially financed by CONICET funds granted to J.R. and by several grants from The Planetary Society, Pasadena, California, U.S.A., to M.R. The authors are greatly indebted to Dr. William MacDonald, State University of New York at Binghamton, USA, for enlightening comments during his recent visit to Ushuaia, to Dr. Sergio Matheos and CIG (La Plata) for the X-ray studies, and to Dr. Adriana Ocampo, Dr. Jack Vitek and Dr. Edgardo Latrubesse, Dr. Guido Ventura and anonymous reviewers for their comments on previous drafts of the manuscript, which significantly improved it. Nonetheless, all possible errors that may be present in this paper are of our responsibility.

References

Aaloe, A.O., Tiirmaa, R.T., 1982. Meteoritic matter in and around the small craters of Kaalijarvi. Meteoritika 41, 120–125 (In Russian).

Aaloe, A.A., Korchemagin, V.A., Osadchiy, Ye.G., Tsvetkov, V.I., 1974. Some characteristics of jointing in craters produced by the Sikhote–Alin meteorite shower. Doklady Akademii Nauk SSSR 215, 409–412 (In Russian).

Alderman, A.R., 1931. The meteorite craters at Henbury, central Australia, with addendum by L.J. Spencer. Mineralogical Magazine (London) 23, 19–32.

Ardolino, A.A., 1981. El vulcanismo cenozoico del borde suroccidental de la meseta de Somún Curá, provincia del Chubut. *Actas VIII Congreso Geológico Argentino* I, 65 (Tabla); III, 7-23. Buenos Aires.

Ardolino, A.A., 1987. Descripción Geológica de la Hoja 42f. Sierra de Apas, Provincia de Chubut. Servicio Geológico Nacional. Dirección Nacional de Minería y Geología. (Buenos Aires, 91 pp.).

Ardolino, A.A., Franchi, M., 1996. Hoja Geológica 4366-1. Telsen. Dirección Nacional del Servicio Geológico, Subsecretaría de Minería de la Nación, Boletín 215. (Buenos Aires, 110 pp.).

Axon, H.J., Steele-Perkins, E.M., 1975. Fracture mechanism of Henbury meteorite by separation along surfaces of shear faulting. Nature 256, 635.

Bartoschewitz, R., 2002. Morasko. The largest known meteorite strewn field? Meteorite 8, 20.

Bunch, T.E., Cassidy, W.A., 1968. Impact-induced deformation in Campo del Cielo meteorite. In: French, B.M., Short, N.M. (Eds.), Shock Metamorphism of Natural Materials. Mono Book Corp., Baltimore, MD, pp. 601–612.

Campins, H., Fernández, Y., 2002. Observational constraints on surface characteristics of comet nuclei. Earth Moon and Planets 89, 117–134.

Cassidy, W.A., 1968. Meteorite impact craters at Campo del Cielo, Argentina. In: French, B.M., Short, N.M. (Eds.), Shock Metamorphism of Natural Materials. Mono Book Corp., Baltimore, MD, pp. 117–128.

Cassidy, W.A., 1971. A small meteorite crater: structural details. Journal of Geophysical Research 76, 3896–3912.

Cassidy, W.A., Renard, M.L., 1996. Discovering research value in the Campo del Cielo, Argentina, meteorite craters. Meteoritics & Planetary Science 31, 433–448.

Cassidy, W.A., Wright, S.P., 2003. Small impact craters in Argentine loess: a step-up from modeling experiments. Impact Cratering Workshop, Houston, February 2003, Texas, USA, p. 8004.

Cassidy, W.A., Villar, L.M., Bunch, T.E., Kohman, T.P., Milton, D.J., 1965. Meteorites and craters of Campo del Cielo, Argentina. Science 149, 1055–1064.

Chappelow, J.E., Sharpton, V.L., 2002. An improved shadow measurement technique for constraining the morphometry of simple impact craters. Meteoritics and Planetary Science 37 (4), 479–486.

Compston, W., Taylor, S.R., 1969. Rb–Sr study of impact glass and country rocks from the Henbury meteorite crater field. Geochimica et Cosmochimica Acta 33, 1037–1043.

Corbella, H., 1987. Agrupamiento de cráteres por posible impacto. Bajada del Diablo, Provincia del Chubut, Argentina. *Revista de la Asociación Argentina de Mineralogía, Petrología y Sedimentología (AMPS)* 18, 1-4, 67. Buenos Aires.

Divari, N.B., 1962. Estimate of the impact velocities of some specimens of the Sikhote-Alin multiple fall. Meteoritika 22, 31–41 (In Russian).

El-Baz, F., El Goresy, A., 1971. Al-Hadida and Um-Hadid Meteorites, Saudi Arabia. Meteoritics 6 (4), 265–266.

Fedynsky, V.V., Khryanina, L.P., 1976. The probable number of meteorite craters in the USSR. Astronomicheskii Vestnik 10, 81–87 (In Russian).

Fesenkov, V.G., 1958. A few thoughts on the energy of crater-formation and the fall velocity of the Sikhote-Alin meteorite. Meteoritika 16, 147–155 (In Russian).

Festou, M.C., Keller, H.U., Weaver, H.A., 2004. Comets 2. University of Arizona Press, Tucson. (745 pp.).

Fisher, D.E., 1963. Ages of the Sikhote Alin iron meteorite. Science 139, 752–753.

Fredriksson, K., Dube, A., Milton, D.J., Balasundaram, M.S., 1973. Lonar Lake, India: an impact crater in basalt. Science 180, 862–864.

Fujiwara, A., Kawaguchi, J., Yeomans, D.K., Abe, M., Mukai, T., Okada, T., Saito, J., Yano, H., Yoshikawa, M., Scheeres, D.J., Barnouin-Jha, O., Cheng, A.F., Demura, H., Gaskell, R.W., Hirata, N., Ikeda, H., Kominato, T., Miyamoto, H., Nakamura, A.M., Nakamura, R., Sasaki, S., Uesugi, K., 2006. The rubble-pile asteroid Itokawa as observed by Hayabusa. Science 312 (5778), 1330–1334.

González Díaz, E., Malagnino, E.C., 1984. Geomorfología. Relatorio IX Congreso Geológico Argentino (Buenos Aires, pp. 347-364).

Hodge, P.W., 1965. The Henbury meteorite craters. Smithsonian Contributions, Astrophysics 8, 199–201.

Hodge, P.W., Wright, F.W., 1971. Meteoritic particles in the soil surrounding the Henbury meteorite craters. Journal of Geophysical Research 76, 3880–3895.

Kestlane, Yu.V., Tsvetkov, V.I., 1987. Sikhote-Alin meteor craters. XX All-Union Meteorite Conference, Tallinn, Estonia, p. 68 (In Russian).

Kolesnikov, E.M., Lavrukhina, A.K., Fisenko, A.V., Levsky, L.K., 1972. Radiation ages of different fragments of the Sikhote-Alin meteorite fall. Geochimica et Cosmochimica Acta 36, 573–576.

Krinov, E.L., 1961. The Kaalijarv meteorite craters on Saarema Island, Estonian SSR. American Journal of Science 259, 430–440.

Krinov, E.L., 1963. The Tunguska and Sikhote-Alin meteorites. In: Middlehurst, B.M., Kniper, G.D. (Eds.), The Moon, Meteorites and Comets. University of Chicago Press, Chicago, IL, pp. 208–234.

Krinov, E.L., 1966. The Silhote-Aline iron meteorite shower. In: Beynon, M.M. (Ed.), Giant Meteorites. Pergamon Press, New York, pp. 266–376.

Krinov, E.L., 1971. New studies of the Sikhote-Alin iron meteorite shower. Meteoritics 6, 284–285.

Krinov, E.L., 1972. Four years of new investigations of the fall and accumulation of fragments of the Sikhote-Alin meteorite shower. Meteoritika 31, 62–67 (In Russian).

Krinov, E.L., 1975. The fragmentation of the Sikhote-Alin meteorite shower. Meteoritika 34, 3–14 (In Russian).

Lyakhovitskiy, F.M., Guklengov, M.N., 1987. Seismic prospecting in Kaali meteor craters: results and prospects. XX All-Union Meteorite Conference, Tallinn, Estonia, pp. 46–47 (In Russian).

Marini, F., Raukas, A., Tiirmaa, R., 2004. Magnetic fines from the Kaali impact-site (Holocene, Estonia): preliminary SEM investigation. Geochemical Journal 38, 107–120.

McColl, D., 1990. Distribution and sculpturing of iron meteorites from the major craters at Henbury (abstract). Meteoritics 25, 384.

McColl, D., 1997. Henbury iron meteorites. Meteorite! 3, 8–10.

McHone, J.F., Killgore, M., 1998. Impact-produced surface craters on Sikhote-Alin irons. Meteoritics and Planetary Science 33 (4), A101–A102.

Melosh, H.J., Ivanov, B.A., 1999. Impact crater collapse. Annual Review of Earth and. Planetary Sciences 27, 385–415.

Millman, P.M., 1970. Current research at Sikhote-Alin. Journal of the Royal Astronomical Society of Canada 64, 251–253.

Milton, D.J., 1964. The Campo del Cielo Meteorite Crater Field, Argentina. U.S. Geological Survey, Astrogeologic Studies Annual Progress Report. U.S.G.S., Washington D.C. , pp. 91–97.

Milton, D.J., 1968. Structure of the Henbury meteorite craters, Australia. In: French, B.M., Short, N.M. (Eds.), Shock Metamorphism of Natural Materials. Mono Book Corp, Baltimore, MD, pp. 115–116.

Milton, D.J., 1972. Structural geology of the Henbury Meteorite Craters, Northern Territory, Australia. U.S. Geological Survey Professional Paper 599-C, Washington D.C., C1–C17.

Milton, D.J., Michel, F.C., 1965. Structure of a ray crater at Henbury, Northern Territory, Australia. U.S. Geological Survey Professional Paper 525-C, Washington D.C., C5–C11.

Nágera, J.J., 1926. Los Hoyos del Campo del Cielo y el Meteorito. *Dirección General de Minas, Geología e Hidrología, Publicaciones*, 19, Buenos Aires.

Nekrasov, V.I., Tsvetkov, V.I., 1970. Present state of the craterlets and craters and the Sikhote-Alin meteor shower. Meteoritika 30, 28–52 (In Russian).
O'Keefe, J.A., 1980. Comments on chemical relationships among irghizites, zhamanshinites, Australasian tektites and Henbury impact glass. Geochimica et Cosmochimica Acta 44, 2151–2152.
O'Keefe, J.D., Ahrens, T.J., 1999. Complex craters: Relationship of stratigraphy and rings to impact conditions. Journal of Geophysical Research 104(E11), 27,091–27,104.
Paillou, P., El Barkooky, A., Barakat, A., Malezieux, J.M., Reynard, B., Dejax, J., Heggy, E., 2004. Discovery of the largest impact crater field on Earth in the Gilf Kebir region, Egypt. Geoscience 336, 1491–1500.
Philby, H.St.J.B., 1933. The Empty Quarter. Henry Holt & Co, New York. 432 pp.
Rayner, J.M., 1939. Examination of the Henbury meteorite craters by the methods of applied geophysics. In: Walkom, U. (Ed.), Australian and New Zealand Association Advancement of Science Report, vol. 24. Australia, Adelaide, pp. 72–78.
Schüssler, U., Rappenglück, M.A., Ernstson, K., Mayer, W., Rappenglück, B., 2005. Das Impakt-Kraterstreufeld im Chiemgau. European Journal of Mineralogy 17 (1), 124 (In German).
Shkerin, L.M., 1973. Results of the petrotectonic study of rocks from the Sikhote-Alin meteorite crater No. 1. Geotectonika 4, 109–115 (In Russian).
Shoemaker, E.M., Wynn, J.C., 1997. Geology of the Wabar meteorite craters, Saudi Arabia. Proceedings of the XXVIII Lunar and Planetary Science Conference, Houston, Texas, 17-21 March, pp. 1313–1314.
Simmons, K., 1975. Australia's Henbury craters. Sky and Telescope 49, 287–290.
Spencer, L.J., Hey, M.H., 1933. Meteoric iron and silica-glass from the meteorite craters of Henbury (central Australia) and Wabar (Arabia). Mineralogical Magazine 23, 387–404.
Taylor, S.R., 1965. Similarity in composition between Henbury impact glass and australites. Geochimica et Cosmochimica Acta 29, 599–601.
Taylor, S.R., 1966. Australites, Henbury impact glass and subgreywacke: a comparison of the abundances of 51 elements. Geochimica et Cosmochimica Acta 30, 1121–1136.
Taylor, S.R., 1967. Composition of meteorite impact glass across the Henbury strewn field. Geochimica et Cosmochimica Acta 31, 961–968.
Taylor, S.R., Kolbe, P., 1964. Henbury impact glass–parent material and behavior of volatile elements during melting. Nature 203, 390–391.
Taylor, S.R., Kolbe, P., 1965. Geochemistry of Henbury impact glass. Geochimica et Cosmochimica Acta 29, 741–745.
Taylor, S.R., McLennan, S.M., 1979. Chemical relationships among irghizites, zhamanshinites, Australasian tektites and Henbury impact glasses. Geochimica et Cosmochimica Acta 43, 1551–1565.
Traub, S.G., Cassidy, W.A., 1989. Alteration of Campo Del Cielo soil by meteorite impact: implications for the surface of Mars. Lunar and Planetary Science 20, 1128–1129.
Tsvetkov, V.I., 1972. Relationship between the fragmentation and distribution of the Sikhote-Alin meteorite shower and the structure of the meteorite. Astronomicheskii Vestnik 17, 122–126 (In Russian).
Villar, L.M., 1968. La dispersión meteorítica en la Argentina y Chile. Ciencia e Investigación 302–314 (July 1968, Buenos Aires).
Wright, S.P., Vesconi, M.A., Spagnuolo, M.G., Cerutti, C., Jacob, R.W., Cassidy, W.A., 2007. Explosion craters and penetration funnels in the Campo del Cielo, Argentina crater field. Lunar and Planetary Science 38, 2017.
Wynn, J.C., 2002. Mapping Armageddon with a magnetometer - the Wabar impact site at 61 °C. Proceedings of the Environmental & Engineering Geophysical Society, Las Vegas, NV, February 10-14, 14 pages, 9 figures (CD-ROM).
Wynn, J.C., Shoemaker, E.M., 1997. Secrets of the Wabar Craters. Sky & Telescope Magazine. (November, 44-48).